Journal of Materials Chemistry A

Accepted Manuscript

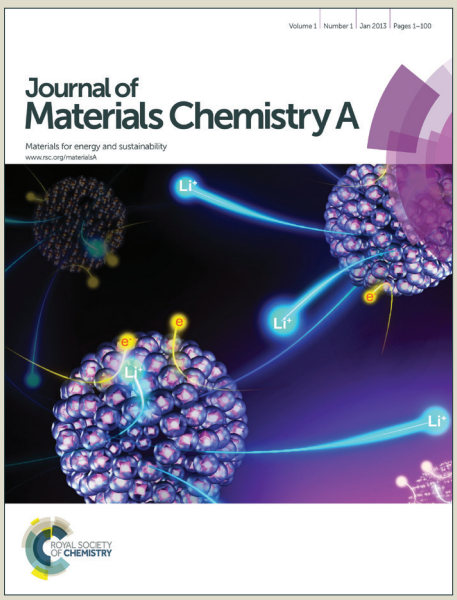

This is an *Accepted Manuscript*, which has been through the Royal Society of Chemistry peer review process and has been accepted for publication.

Accepted Manuscripts are published online shortly after acceptance, before technical editing, formatting and proof reading. Using this free service, authors can make their results available to the community, in citable form, before we publish the edited article. We will replace this *Accepted Manuscript* with the edited and formatted *Advance Article* as soon as it is available.

You can find more information about *Accepted Manuscripts* in the Information for Authors.

Please note that technical editing may introduce minor changes to the text and/or graphics, which may alter content. The journal's standard Terms & Conditions and the Ethical guidelines still apply. In no event shall the Royal Society of Chemistry be held responsible for any errors or omissions in this *Accepted Manuscript* or any consequences arising from the use of any information it contains.

ROYAL SOCIETY OF CHEMISTRY

www.rsc.org/materialsA

TOC

One-Pot Route to Alloyed Cu/Ag Bimetallic Nanoparticles with Different Mass Ratio for Catalytic Reduction of 4-Nitrophenol

W. Wu, M. Lei, S. L. Yang, L. Zhou, L. Liu, X. H. Xiao, C. Z. Jiang, V. A. L. Roy**

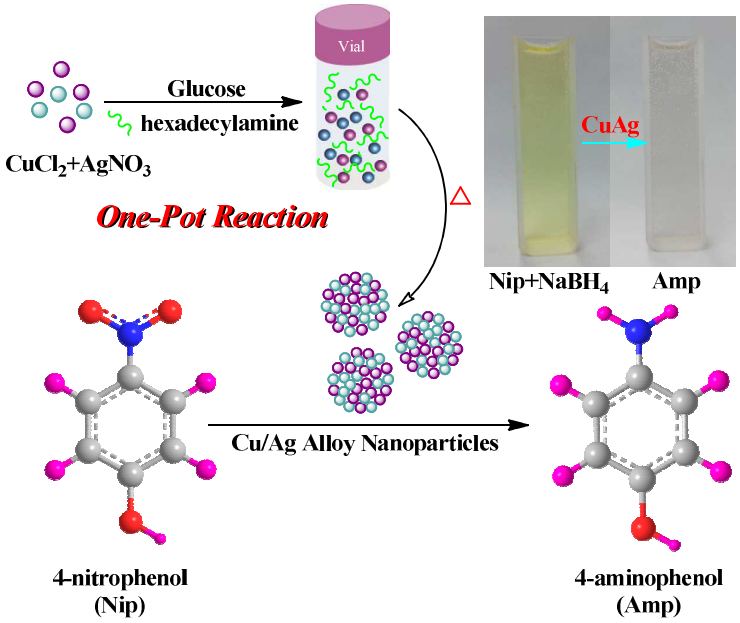

Journal of Materials Chemistry A Accepted Manuscript

One-Pot Route to Alloyed Cu/Ag Bimetallic Nanoparticles for Catalytic Reduction of 4-Nitrophenol

Wei Wu[1,2], Mei Lei[3], Shuanglei Yang[4], Li Zhou[2], Li Liu[1], Xiangheng Xiao[3], Changzhong Jiang[3], Vellaisamy A.L. Roy[2]**

[1] Laboratory of Printable Functional Nanomaterials and Printed Electronics, School of Printing and Packaging, Wuhan University, Wuhan 430072, P. R. China

[2] Department of Physics and Materials Science and Center of Super-Diamond and Advanced Films (COSDAF), City University of Hong Kong, Hong Kong SAR, P. R. China

[3] Key Laboratory of Artificial Micro- and Nano-structures of Ministry of Education, School of Physics and Technology, Wuhan University, Wuhan 430072, P. R. China

[4] State Key Laboratory for Powder Metallurgy, Central South University, Changsha 410083, P. R. China

Corresponding authors: weiwu@whu.edu.cn (W. Wu) and val.roy@cityu.edu.hk (V.A.L. Roy)

Abstract

Copper-based alloy nanoparticles (NPs) have recently triggered various research interests for the development of low-cost and high-performance bimetallic catalysts that have industrial applications. Here, we present alloyed Cu/Ag bimetallic NPs synthesized by a facial one-pot reduction method. The catalytic property of these prepared Cu/Ag bimetallic NPs with different ratio have been investigated by reducing 4-nitrophenol (Nip) into 4-aminophenol (Amp) in the presence of $NaBH_4$. In comparison with pristine Ag monometallic NPs, alloyed Cu/Ag bimetallic NPs exhibit high catalytic performance on the reduction of Nip. The current synthesis method of Cu/Ag bimetallic NPs does not require rigorous

Journal of Materials Chemistry A Accepted Manuscript

conditions or toxic agents, and thus it is a rapid, efficient, and green approach for the fabrication of active bimetallic catalysts.

Keywords: Cu/Ag; bimetallic NPs; alloyed NPs; catalytic application

1. Introduction

Bimetallic NPs constructed from more than one metallic phase have attracted interest to an increasing degree during recent years because of their intriguing properties and potential use in catalysis, electronics, photonics, sensing, labelling and imaging.[1-3] In many cases, bimetallic alloy NPs have higher catalytic efficiencies than their monometallic counterparts, owing to strong synergistic effects between the two metals. In order to form alloyed bimetallic nanocrystals, the two distinct metal atoms have a homogeneous distribution in one particle, thus the reaction kinetics must be rigidly controlled.[4] Although many literatures have focused on the preparation of bimetallic alloyed NPs, such as Au/Ag, Au/Pt, reports on bimetallic particles of Cu/Ag are scarce so far. Because of the lattice constants of Cu (0.409 nm) and Ag (0.361 nm) is different and that makes the synthesis of their alloy difficult.[5] Various approaches, such as wet-chemical reduction, microemulsion, microwave and sonochemical methods,[6-10] have been developed to synthesize Cu/Ag alloyed NPs because of the diversity and importance of these applications.[11-15]

As a competitive alternative, there has been a shift towards the development of simple, green methods for fabricating bimetallic alloyed NPs. Herein, a facile one-pot reaction strategy was developed to synthesize the uniform Cu/Ag alloy nanostructures. Most important rule in designing green nanomaterial synthesis is the efficiency, i.e. design for materials and energy efficiency. In contrast to the typical two-step strategies or polyol process,[16-18] the current synthesis method is simple and a green approach to produce the Cu/Ag bimetallic NPs. The influences on the addition of copper precursors on the morphology and composition of final product have also been investigated. Finally, the catalytic property of the as prepared Cu/Ag bimetallic NPs have been studied by reducing Nip into amp in the presence of $NaBH_4$ as a model reaction. The current one-pot reaction strategy is an easy scale-up and

Journal of Materials Chemistry A Accepted Manuscript

environmentally friendly method. We envision that the current one-pot reaction strategy can be a guide to synthesize other bimetallic NPs and bimetallic NPs-based catalytic materials.

2. Experimental Sections

2.1 ***Materials.*** Cupric chloride dihydrate ($CuCl_2 \cdot 2H_2O$, AR), glucose (AR), silver nitrate ($AgNO_3$, AR), hexadecylamine ($CH_3(CH_2)_{15}NH_2$, AR) and 4-nitrophenol ($O_2NC_6H_4OH$, AR) were purchased from Sigma-Aldrich. All chemicals used as received without further purification.

2.2 ***Synthesis of Cu/Ag bimetallic alloy NPs.***

6 mL of silver nitrate aqueous solution (20 mM) was added into a vial, and then a certain amount of $CuCl_2$ (0, 9, 18 and 27 mg), 180 mg of hexadecylamine and 50 mg of glucose were added, the mixture was magnetically stirred for 5 h. Subsequently, the mixture was heated at 100 ºC for 2 h under vigorous stirring (300 r/min). The resulted products were collected by centrifugation and washed several times.

2.3 ***Characterization.*** Transmission electron microscopy (TEM), high-resolution TEM (HRTEM), and energy-dispersive X-ray (EDX) spectroscopy were carried out by a JEOL JEM-2100F transmission electron microscope at 200 kV. The high angle annular dark field-scanning transmission electron microscopy (HADDF-STEM) images and EDX mapping of Cu/Ag nanoparticles were performed on the FEI Tecnai G2 F20 transmission electron microscope. The samples were dissolved in water and dropped on nickel (Ni) grids for TEM inspection. UV-Vis measurements were conducted on a Shimadzu 2550 spectrophotometer.

2.4 Catalytic reduction of Nip. The catalytic reduction of Nip was studied using a standard quartz cuvette by adding 150 μL of $NaBH_4$ (0.3 M) to 4 mL of Nip (0.1 mM). Then 2 mg of sample was added into the solution and time-dependent absorption spectra was recorded at room temperature with a time interval of 60 s and a range of 200 to 500 nm. With constant magnetic stirring, the green yellow solution became colorless. The total reaction progress and UV-vis spectra of the starting material, Nip and the product Amp was recorded by Shimadzu 2550 spectrophotometer, which shows different absorption in the UV-visible region.

Journal of Materials Chemistry A Accepted Manuscript

3. Results and Discussion

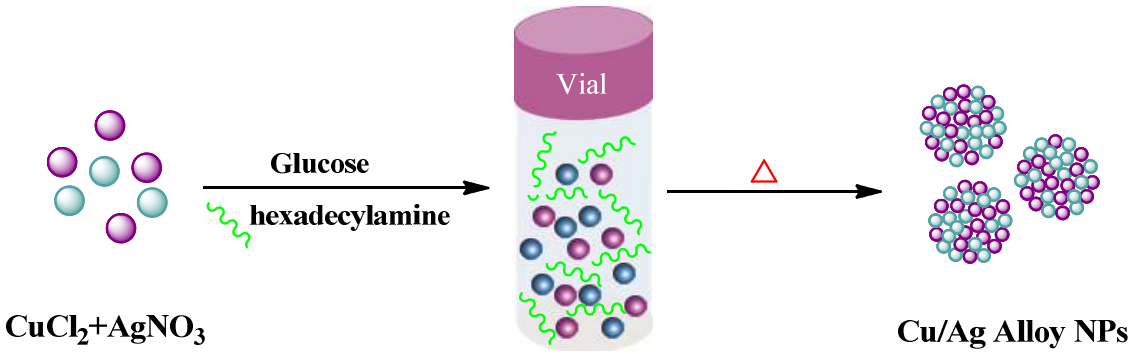

Figure 1 Schematic illustration of the one-pot synthetic procedure of Cu/Ag bimetallic NPs.

As shown in **Figure 1**, a one-pot method is developed for the synthesis of alloyed Cu/Ag bimetallic NPs. Silver nitrate and cupric chloride are used as Ag and Cu precursor, respectively. Low-cost glucose is used as a reducing agent, and hexadecylamine (HDA) is used as a selective capping agent for the {100} facets of Cu.[19, 20] Ring-opening process of glucose generates aldehyde, which reduces the Ag^+ to Ag^0. However, the generated aldehyde glucose is disordered at room temperature in an equilibrium reaction, thus it is difficult to reduce Ag^+ to Ag^0.[21] Therefore, the reaction of Cu^{2+} with glucose (capable of reducing Cu^{II} into Cu^0) forms Cu NPs. Because of the single galvanic replacement reaction of $Cu + 2Ag^+ \rightarrow Cu^{2+} + 2Ag$, the Cu/Ag bimetallic NPs are formed, and thus the amount of Cu precursor is an important parameter to obtain Cu/Ag bimetallic NPs with different atomic ratio of Cu and Ag. In order to get the Cu/Ag bimetallic NPs, excess amount of Cu precursor has been used. In this work, the mole ratio for the amount of Cu and Ag precursor is close to 1:2 (Cu^{2+} = 9 mg), 1:1 (Cu^{2+} = 18 mg) and 2:1 (Cu^{2+} = 27 mg), respectively. Moreover, the subsequent heating process (100 ºC) is to accelerate the generation of aldehyde glucose and the total reaction rate.

Journal of Materials Chemistry A Accepted Manuscript

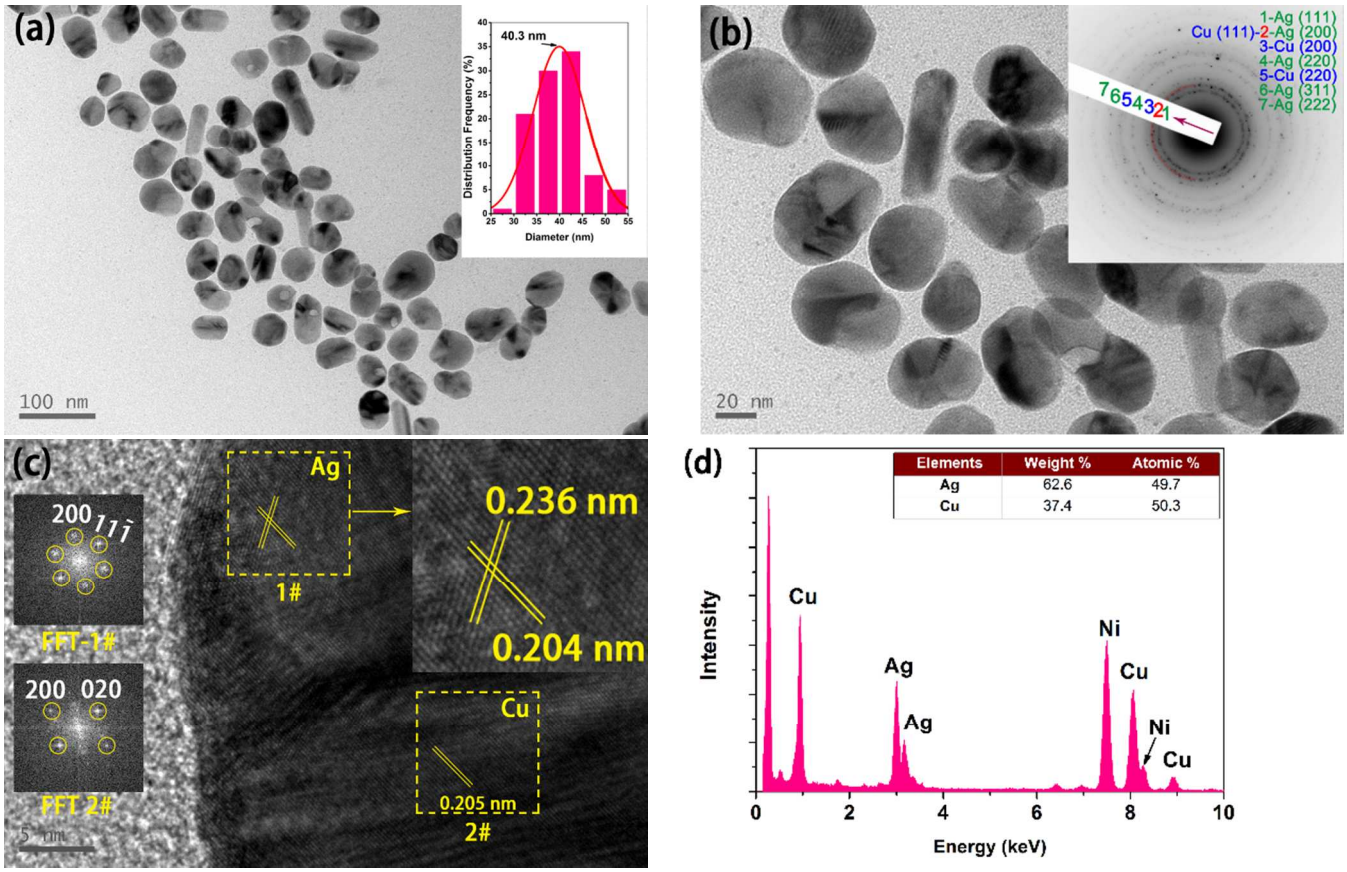

Figure 2 (a) TEM images of Cu/Ag bimetallic NPs at low magnification (Cu = 18 mg), the insert is the histogram of size distribution; (b) TEM images of Cu/Ag bimetallic NPs at higher magnification, the insert is the corresponding selected area electron diffraction pattern; (c) HRTEM image of single Cu/Ag bimetallic NPs, the insert are the corresponding FFT patterns from 1# and 2# area, respectively; (d) the EDX spectra of individual Cu/Ag bimetallic NPs (Ni elemental signal comes from the Ni grid).

Figure 2a and **2b** shows the representative TEM images of as-obtained Cu/Ag alloy NPs, which show that the product consist of uniform spheroidal NPs. The histogram (insert of **Figure 2a**) shows the nanostructures had an average diameter of 40.3 nm. The crystalline nature of the Cu/Ag alloy NPs is confirmed by SAED patterns (the insert of **Figure 2b)**, the (111), (200), (220), (311), and (222) rings are indexed to face-centered cubic (*fcc*) crystal structure of Ag, and the (111), (200) and (220) rings are attributed to *fcc* crystal structure of Cu, respectively. To further identify the alloy nanostructure, we used HRTEM and EDX to analyse the structures and characterize the chemical composition of individual nanoparticle. As shown in **Figure 2c**, two groups of lattice fringes are readily resolved, the lattice distances are 0.236 and 0.204 nm, which can be indexed as (111) and (222) crystal planes of Ag,

Journal of Materials Chemistry A Accepted Manuscript

respectively. Moreover, a clear lattice distance of 0.205 nm can be indexed to the (111) plane of Cu. Similar results were obtained from fast Fourier transform (FFT) analysis. HRTEM results revealed that the particles are composed of Ag and Cu and both have good crystallinity. Indeed, the interface boundaries between adjacent Cu and Ag are readily resolved as shown in **Figure 2c**. **Figure 2d** reveals the existence of Cu and Ag elements in a single particle. And the concentration of Cu and Ag is 50.3 % and 49.7 %, respectively. Thus, the above results fully confirm the successful synthesis of Cu/Ag bimetallic NPs.

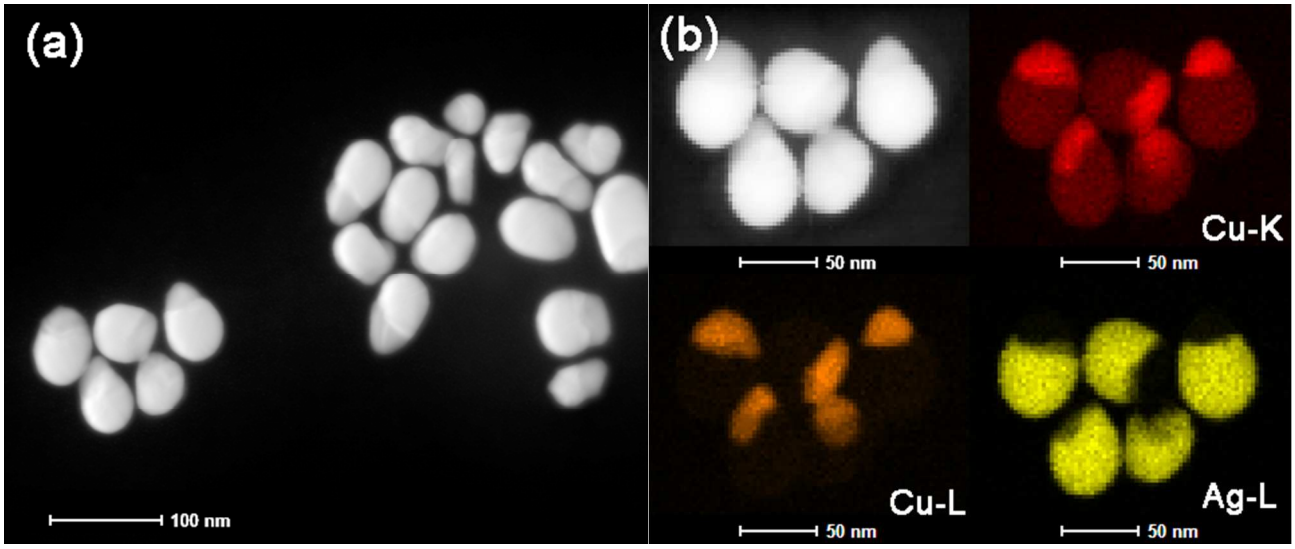

Figure 3 (a) HADDF-STEM image of Cu/Ag bimetallic NPs; (b) Elemental mapping images of Cu/Ag bimetallic NPs, where Cu-K, Cu-L and Ag-L elements are displayed, respectively.

To further identify the as-obtained Cu/Ag bimetallic NPs is alloyed nanostructure, the HADDF-STEM images and EDX elemental mapping analysis have been carried out. **Figure 3a** shows the HADDF-STEM image of Cu/Ag bimetallic NPs, the Z value of Cu (Z = 29) and Ag (Z = 47) is appreciably different, and hence the nanoparticle structure can be determined by the contrast of the image. **Figure 3b** shows the elemental mapping of Cu/Ag bimetallic NPs, the results illustrate that Cu and Ag atoms have a homogeneous distribution in one particle, which formed the alloy structure.

Journal of Materials Chemistry A Accepted Manuscript

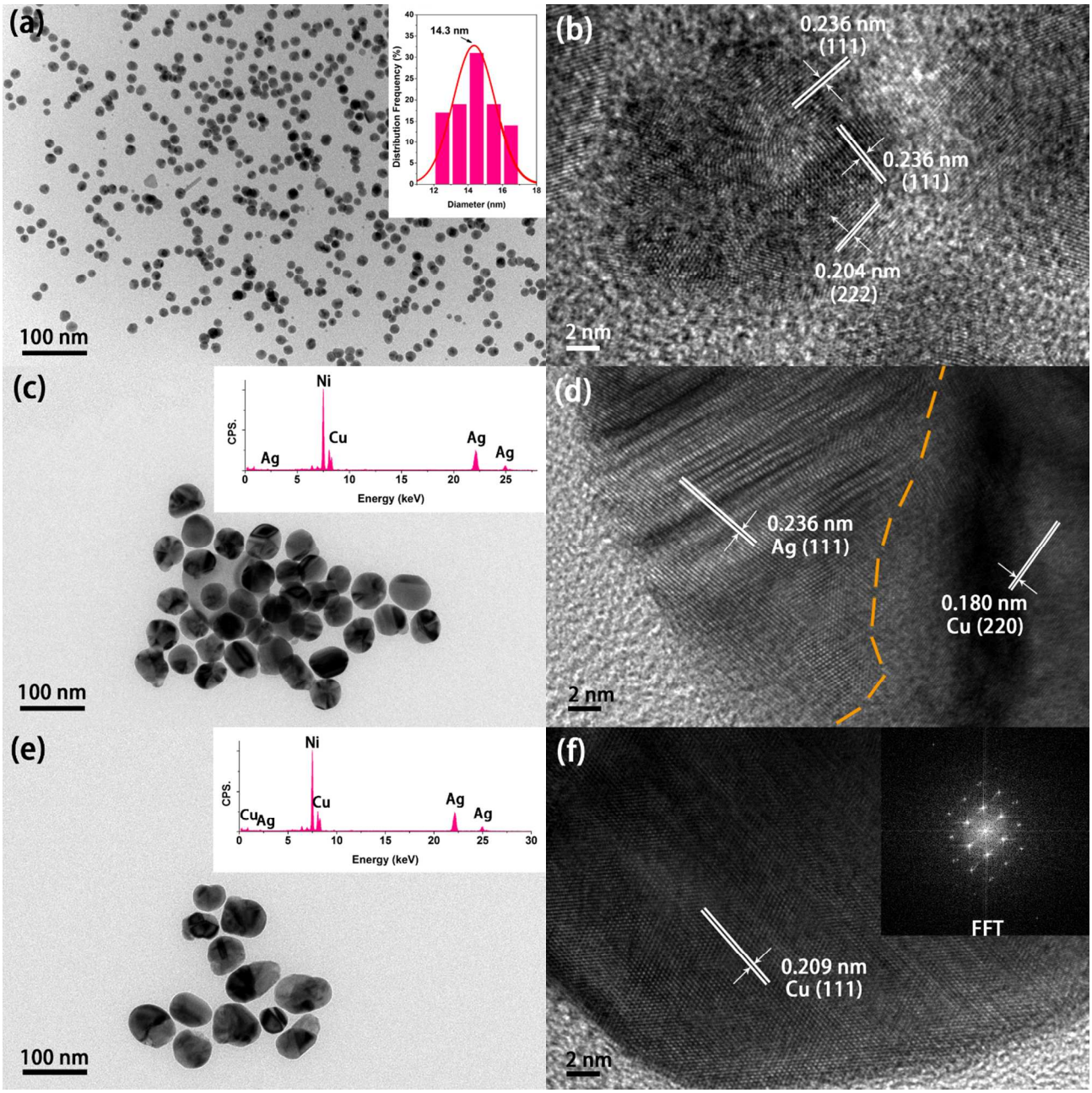

Figure 4 TEM (a) and HRTEM (b) images of Ag NPs at low magnification (Cu = 0 mg), the insert is the histogram of size distribution; TEM (c) and HRTEM (d) images of Cu-Ag bimetallic NPs at low magnification (Cu = 9 mg), the insert is the EDX spectra; TEM (e) and HRTEM (f) images of Cu/Ag bimetallic NPs at low magnification (Cu =27 mg), the insert is the EDX spectra.

Subsequently, experiments have been carried out to understand the dependence of copper precursor on the morphology evolution of Cu/Ag bimetallic nanostructures. If the Cu precursor is absent (0 mg), the as-obtained products are the sub-20 nm Ag NPs. **Figure 4a** shows these Ag NPs have a spherical morphology, the size distribution is narrow and the average diameter is 14.3 ±2.2 nm. **Figure 4b** is the

Journal of Materials Chemistry A Accepted Manuscript

HRTEM image of the as-prepared Ag NPs, and the fringe spacing is measured to be 0.236 nm and 0.204 nm, which corresponds to the spacing between (111) and (222) planes of the *fcc* silver. When the Cu precursor is introduced with an amount of 9 mg, the obtained product becomes Cu/Ag bimetallic NPs. As shown in **Figure 4c**, the size of the product clearly increases and, the shape of NPs is similar to sphere. The EDX reveals the composition of single particle as Ag and Cu. In **Figure 4d**, two groups of lattice fringes are resolved with the lattice distances of 0.236 and 0.180 nm, which corresponds to (111) plane of Ag and (220) plane of Cu, respectively. When the doping amount of Cu precursor is elevated to 27 mg, the shape of NPs still remains as sphere, and the size of NPs becomes 85 nm (**Figure 4e**). Clearly, the size of products depends on the amount of Cu precursor. The EDX reveals the presence of Ag and Cu elements in the single particle with the concentration of Ag and Cu as 1.10 at% and 98.9 at%, respectively. We investigated numerous Cu/Ag NPs by HRTEM, and the representative HRTEM image is shown in **Figure 4f.** The fringe spacing is measured to be 0.209 nm and in combination with FFT pattern, the planes are indexed as (111) planes of the copper. At high concentration of Cu precursor (27 mg), the lattice plane of Ag almost disappears. The results illustrate that Cu precursor is an important parameter to obtain Cu/Ag bimetallic NPs with different atomic ratio of Cu and Ag. TEM images enumerates that the NPs are homogeneous without substantial agglomeration. According to TEM analysis, it can be seen that the average size of the Cu/Ag alloy NPs increases with the concentration of Cu precursor. On the other hand, we were not able to obtain nanosized pure Cu particles in the absence of Ag ions.

Journal of Materials Chemistry A Accepted Manuscript

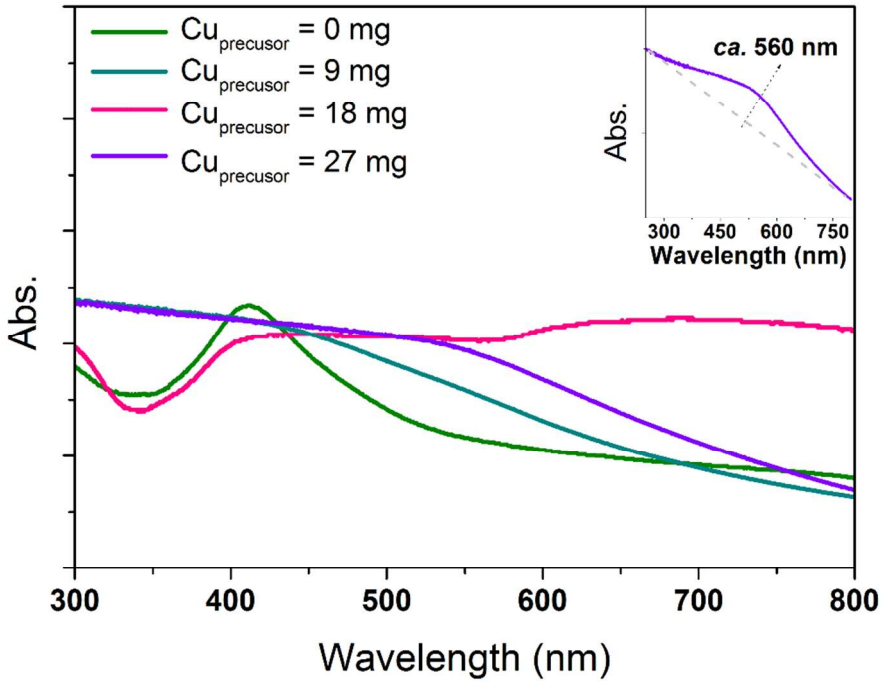

Figure 5 UV-vis absorption spectra of the as-obtained samples with different using amount of copper precursor

Owing to the surface plasmon resonance effect, metal NPs possess collective oscillation of surface electrons and absorb the visible light. We use UV-visible spectrometer to find out the absorption of metal NPs, and a huge shift is found for the NPs with different Cu precursor.[22] The UV-vis absorption spectra of as-obtained samples with copper precursor from 0 -27 mg is shown in **Figure 5**. The as-obtained monometallic Ag and Cu/Ag NPs show absorption peaks at ca. 410 nm and ca. 560 nm, respectively. The surface plasmon peak of pure Cu NPs has been reported at around 570 nm.[23-25] The as-obtained Cu/Ag alloy NPs exhibit an absorption peak between monometallic Cu and Ag NPs. The above results indicate the coexistence of two elements in one particle and form an alloy structure rather than core-shell structure.[26] Two distinct UV absorption peaks are often found in core-shell structured bimetallic NPs attributed to the signal of each element.[27]

Journal of Materials Chemistry A Accepted Manuscript

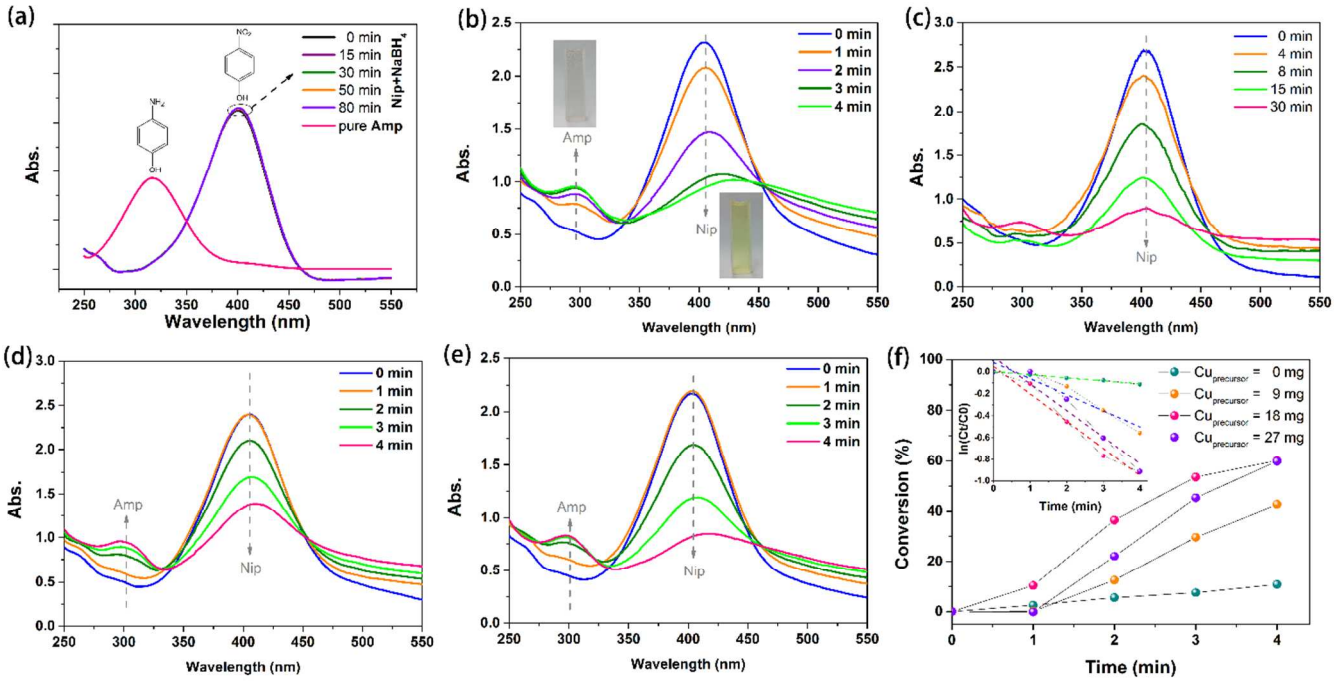

Figure 6 Successive UV–vis absorption spectra for the reduction of 0.1 mM Nip by 0.3 M $NaBH_4$ in the presence of (a) without NPs and pure Amp, (b) bimetallic Cu/Ag NPs ($Cu_{precursor}$ = 18 mg), (c) Ag NPs ($Cu_{precursor}$ = 0 mg), (d) bimetallic Cu/Ag NPs ($Cu_{precursor}$ = 9 mg), and (e) bimetallic Cu/Ag NPs ($Cu_{precursor}$ = 27 mg); Conversion of Nip vs. time (f, the insert is $\ln(C_t/C_0)$ versus reaction time).

The different atomic distribution and ratio can greatly influence the catalytic performance of bimetallic NPs. Therefore, we investigated the catalytic property of the prepared Cu/Ag bimetallic NPs with different ratio by employing them for the reduction of 4-nitrophenol (Nip) into 4-aminophenol (Amp) with $NaBH_4$ as a model reaction at room temperature. The absorption peak of Nip solution is at 317 nm, this peak is red-shifted to 400 nm when $NaBH_4$ is introduced, which comes from the formation of 4-nitrophenolate ions owing to an increase in solution alkalinity upon the addition of $NaBH_4$.[28] As shown in **Figure 6a**, for the control experiment (without metallic NPs presence), there is no change for the peak at 400 nm for 80 minutes, confirming that no reduction takes place without metal NPs. However, this peak starts to decrease and a new peak at 300 nm appears with reaction time due to the presence of Ag and Cu/Ag, suggesting the reduction of Nip. Over the course, with the presence of Cu/Ag NPs ($Cu_{precursor}$ = 18 mg) the peak intensity of 400 nm is rapidly decreased in 4 minutes, and the

Journal of Materials Chemistry A Accepted Manuscript

colour of the solution changes from yellow to transparent (**Figure 6b**). Simultaneously, new peak appears at about 300 nm indicating the generation of Amp.

The UV–vis absorption spectra for the Nip reduction reaction of other samples with different amount of copper precursor are shown in **Figure 6c-e.** The catalytic abilities of as-obtained pure Ag nanoparticles is very weak, and the isosbestic point is disorderly, this is because of pure Ag NPs will generate different reactant diffusion to metallic surface and product diffusion away from particle surface.[28] Clearly, the bimetallic Cu/Ag NPs exhibits significant catalytic activity. The activity of Cu/Ag NPs ($Cu_{precursor}$ = 18 mg) was about 5 times higher than that of as-prepared monometallic Ag NPs. In the catalytic test, the concentration of $NaBH_4$ in all the reactions is fixed at 3000-times higher than that of Nip. Excess amount of reductant $NaBH_4$ was used, in this case, the reduction rate constant can be calculated based on pseudo-first-order kinetics:[29-31] $\ln(C_t/C_0) = \ln(A_t/A_0) = -k_{app}t$, where k_{app} is the apparent rate constant, and C_t and C_0 correspond to the concentration of Nip at time t and its initial concentration, respectively. **Figure 6f** shows the conversion and linear plots of $\ln(C_t/C_0)$ vs. t, which fit well with the first-order reaction kinetics. The k_{app} is calculated based on the slopes of the lines, and the results reveal that the k_{app} value of the products at $Cu_{precursor}$ = 18 mg is 3.95×10^{-3} s^{-1}, which is higher than other samples (the k_{app} value of $Cu_{precursor}$ = 0 mg, 9 mg and 27 mg is 4.70×10^{-4} s^{-1}, 2.10×10^{-3} s^{-1}, 3.46×10^{-3} s^{-1}, respectively). For the bimetallic NPs, the electron density on the surface is higher than the monometallic NPs because electrons transfer from Cu to Ag, which enhances the catalytic activity due to a synergistic electronic effect.[32, 33] The chemisorption strength of organic molecules is an important factor for catalytic reaction, which depend on the d-band center of the metal surface (could be identified by Hammer−Nørskov model,[34-36] and Ag locates at -3.9 eV and Cu locates at -2.4 eV, respectively). When the Nip interacts with the d-band of Ag and Cu, the adsorbate state overlaps with the metal states and is split off into bonding and antibonding interactions. Additionally, the absorption energy of Ag is -0.75 eV and Cu is -1.45 eV, respectively. If the Ag and Cu contact and form as alloyed structure, the charge would be rearranged. The pure Ag has a low reaction rate constant due to its weak binding, however, the Cu/Ag would generate a stronger binding energy and yields a correspondingly faster

Journal of Materials Chemistry A Accepted Manuscript

reaction rate constant due to its higher adsorption energy (according to volcano plot, the value is about -1.1 eV).[37] The structure effects, composite effects, and size effects due to the intimate interactions of two metals is another factor for the enhanced catalytic performance.[38, 39]

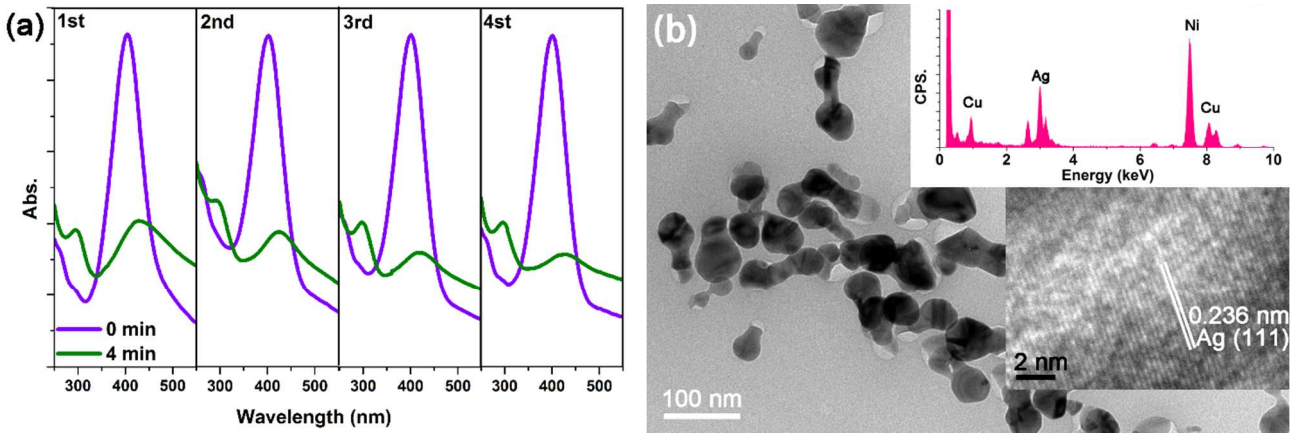

Figure 7 UV–vis absorption spectra for the reduction of 0.1 mM Nip in four cycles (a); TEM image of Cu/Ag NPs after four cycles catalytic test (b, the insert is the EDX spectra and HRTEM of the particles).

As shown in **Figure 7a**, four recycles of the activity were measured for Cu/Ag NPs ($Cu_{precursor}$ = 18 mg) in order to investigate its reusability. The Cu/Ag NPs exhibits similar catalytic performance without significant reduction in the conversion for the same reaction time (4 min), revealing the as-prepared Cu/Ag bimetallic catalysts is stable. After 4 min, the colour of the solution changes from yellow to transparent in all the recycle test. Representative TEM images of the catalysts after four cycles indicate the size, shape and compositions of the Cu/Ag NPs almost remained, further suggesting an excellent stability and long life (**Figure 7b**).

4. Conclusions

In summary, we demonstrate a facile one-pot method for the preparation of well-defined Cu/Ag alloy NPs by using low-cost glucose as a reduction agent. The catalytic activity of the as-prepared alloyed Cu/Ag NPs has been investigated by the catalytic reduction of Nip to Amp. The results reveal that bimetallic Cu/Ag NPs possess higher catalytic activity than as-prepared monometallic Ag NPs. Our simple synthetic method could be extended to prepare other copper-based alloy nanostructures, such as the Cu/Au and Cu/Pt bimetallic NPs, and they are currently under investigation.

Journal of Materials Chemistry A Accepted Manuscript

Acknowledgment

This work was partially supported by the NSFC (51201115, 51471121, 51171132, 11375134), Hong Kong Scholars Program, the Research Grants Council of the Hong Kong Special Administrative Region (Project No.T23-713/11), China Postdoctoral Science Foundation (2014M550406), Hubei Provincial Natural Science Foundation (2014CFB261), Young Chenguang Project of Wuhan City (2013070104010011), the Fundamental Research Funds for the Central Universities and Wuhan University.

References

1. W. Yu, M. D. Porosoff and J. G. Chen, *Chem. Rev.* , 2012, **112**, 5780-5817.
2. M. Sankar, N. Dimitratos, P. J. Miedziak, P. P. Wells, C. J. Kiely and G. J. Hutchings, *Chem. Soc. Rev.* , 2012, **41**, 8099-8139.
3. A. K. Singh and Q. Xu, *ChemCatChem* 2013, **5**, 652-676.
4. X. Liu, D. Wang and Y. Li, *Nano Today*, 2012, **7**, 448-466.
5. M. Valodkar, S. Modi, A. Pal and S. Thakore, *Mater. Res. Bull.* , 2011, **46**, 384-389.
6. M. Tsuji, S. Hikino, R. Tanabe, M. Matsunaga and Y. Sano, *Crystengcomm*, 2010, **12**, 3900-3908.
7. C.-H. Huang, H. P. Wang, J.-E. Chang and E. M. Eyring, *Chem. Commun.* , 2009, 4663-4665.
8. S. Chowdhury, V. R. Bhethanabotla and R. Sen, *J. Phys. Chem. C*, 2009, **113**, 13016-13022.
9. X. Huang, Y. Li, H. Zhou, X. Zhong, X. Duan and Y. Huang, *Chem-Eur J*, 2012, **18**, 9505-9510.
10. S. Chen, S. V. Jenkins, J. Tao, Y. Zhu and J. Chen, *J. Phys. Chem. C*, 2013, **117**, 8924-8932.
11. S. Gamerith, A. Klug, H. Scheiber, U. Scherf, E. Moderegger and E. J. List, *Adv. Funct. Mater.* , 2007, **17**, 3111-3118.
12. E. Butovsky, I. Perelshtein and A. Gedanken, *J. Mater. Chem.* , 2012, **22**, 15025-15030.
13. C. K. Kim, G.-J. Lee, M. K. Lee and C. K. Rhee, *Powder Technol.* , 2014, **263**, 1-6.

Journal of Materials Chemistry A Accepted Manuscript

14. K.-L. Wu, X.-Z. Li, C. Dong, L. Liu, P.-D. Liu, T.-H. Ding, J. Lu and X.-W. Wei, *Chem. Lett.* , 2013, **42**, 1466-1468.

15. J. Zhang, Y. Yuan, X. Xu, X. Wang and X. Yang, *ACS Appl. Mater. Interfaces* 2011, **3**, 4092-4100.

16. M. Tsuji, S. Hikino, R. Tanabe and Y. Sano, *Chem. Lett.* , 2009, **38**, 860-861.

17. M. B. Cortie and A. M. McDonagh, *Chem. Rev.* , 2011, **111**, 3713-3735.

18. M. Miyakawa, N. Hiyoshi, M. Nishioka, H. Koda, K. Sato, A. Miyazawa and T. M. Suzuki, *Nanoscale*, 2014, **6**, 8720-8725.

19. M. Jin, G. He, H. Zhang, J. Zeng, Z. Xie and Y. Xia, *Angew. Chem. Int. Ed.* , 2011, **50**, 10560-10564.

20. M. Jin, H. Zhang, J. Wang, X. Zhong, N. Lu, Z. Li, Z. Xie, M. J. Kim and Y. Xia, *Acs Nano*, 2012, **6**, 2566-2573.

21. T. Tetsumoto, Y. Gotoh and T. Ishiwatari, *J. Colloid Interface Sci.* , 2011, **362**, 267-273.

22. T. M. D. Dang, T. T. T. Le, E. Fribourg-Blanc and M. C. Dang, *Adv. Nat. Sci: Nanosci. Nanotechnol.*, 2011, **2**, 015009.

23. S.-H. Wu and D.-H. Chen, *J. Colloid Interface Sci.* , 2004, **273**, 165-169.

24. J. Xiong, Y. Wang, Q. Xue and X. Wu, *Green Chem.* , 2011, **13**, 900-904.

25. M. Vaseem, K. M. Lee, D. Y. Kim and Y.-B. Hahn, *Mater. Chem. Phys.* , 2011, **125**, 334-341.

26. A. Bansal, J. S. Sekhon and S. Verma, *Plasmonics*, 2014, **9**, 143-150.

27. M. P. Mallin and C. J. Murphy, *Nano Lett.* , 2002, **2**, 1235-1237.

28. Y. Lin, Y. Qiao, Y. Wang, Y. Yan and J. Huang, *J. Mater. Chem.* , 2012, **22**, 18314-18320.

29. X.-Y. Liu, F. Cheng, Y. Liu, H.-J. Liu and Y. Chen, *J. Mater. Chem.* , 2010, **20**, 360-368.

30. S. Firdoz, W. Zhang, W. Niu and X. Lu, *Chem. Phys. Lett.* .

31. X. Gu, W. Qi, X. Xu, Z. Sun, L. Zhang, W. Liu, X. Pan and D. Su, *Nanoscale*, 2014, **6**, 6609-6616.

32. X. Peng, Q. Pan and G. L. Rempel, *Chem. Soc. Rev.* , 2008, **37**, 1619-1628.

Journal of Materials Chemistry A Accepted Manuscript

33. F. Zaera, *Chem. Soc. Rev.* , 2013, **42**, 2746-2762.

34. B. Hammer, Y. Morikawa and J. K. Nørskov, *Phys. Rev. Lett.* , 1996, **76**, 2141.

35. B. Hammer and J. Nørskov, *Surf. Sci.* , 1995, **343**, 211-220.

36. B. Hammer, *Top. Catal.* , 2006, **37**, 3-16.

37. Z. D. Pozun, S. E. Rodenbusch, E. Keller, K. Tran, W. Tang, K. J. Stevenson and G. Henkelman, *J. Phys. Chem. C*, 2013, **117**, 7598-7604.

38. Z. Wei, J. Sun, Y. Li, A. K. Datye and Y. Wang, *Chem. Soc. Rev.* , 2012, **41**, 7994-8008.

39. B. Xia, F. He and L. Li, *Langmuir*, 2013, **29**, 4901-4907.

Journal of Materials Chemistry A Accepted Manuscript